View metadata, citation and similar papers at core.ac.uk
brought to you by CORE
provided by Elsevier - Publisher Connector

Mark Telford

This May's *13th Indium Phosphide and Related Materials* conference (IPRM'01) in Nara, Japan attracted a record 470 delegates, despite the slowdown in the industry (perhaps due to it mainly hitting the GaAs sector) and there being few delegates from travel-restricted companies like Lucent and Agilent. As well as advances such as monolithically grown and integrated MEMS-tunable VCSELs, reports included the extension of more temperature-stable materials than InP (such as GaInNAs) to 1.55 pm lasers for the first time, as well as advances in InP electronics and metamorphic GaAs-based devices.

Advances in InP and competing materials

1. Monolithic and tunable long-wavelength lasers

Currently, 1.3 and 1.55 μm fibre-optic transmission is provided by InP-based edge-emitting lasers. However, vertical cavity surface emitting lasers (VCSELs) have intrinsic advantages over edge-emitting lasers, such as sub-milliAmp threshold currents, low beam divergence, simple fibre coupling and pre-packaging wafer-level testing, high slope efficiencies and low power consumption, as well as the established use of GaAs-based VCSELs at 850-950 nm. It is therefore desirable to extend their use to long-wavelengths (1.3-l. 55 μm) for medium- to long-range fibre-optic data communications or environmental gas sensing.

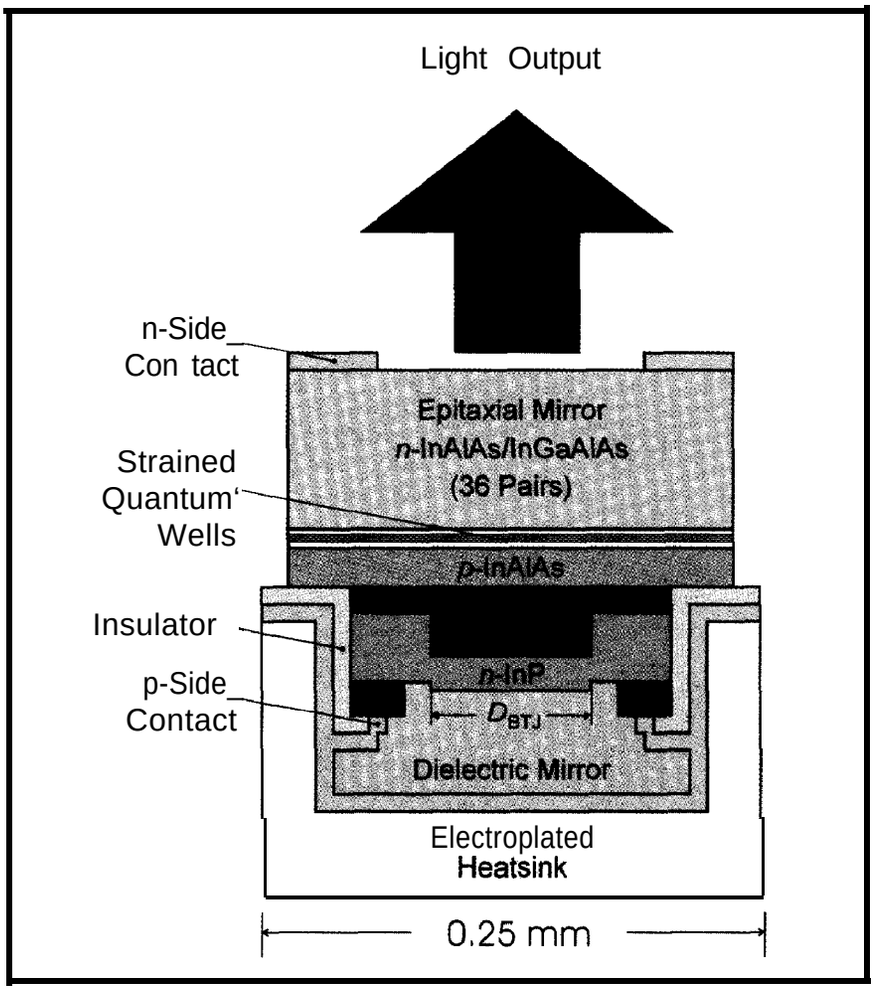

Figure 1. Schematic cross section of InP-based buried tunnel junction VCSEL.

However, long-wavelength VCSELs suffer from smaller index contrast and thermal conductivity of the mirror layers, stronger temperature dependence of the optical gain, and difficulties for self-aligned lateral index and current confinement.

In particular, InP-based VCSELs can require wafer bonding. However, this can be avoided by using a metamorphic buffer or a buried tunnel junction.

Bottom-emitting buried tunnel junctions

M C Amann of the Walter Schottky Institut, Technische Universität München reported monolithic InP-based 1.45-l .85 μm VCSELs based on laterally structured buried tunnel junctions (BTJ-VCSEL - see Figure 1). These have a bottom-emitting structure mounted p-side down with a 99.5-99.8% reflective thin (1.5-layer or 2.5-layer) hybrid gold-dielectric mirror on to an integrated gold heatsink so that the similarly reflective 30-40 layer pair InAlAs/InGa(Al)As mirror does not determine

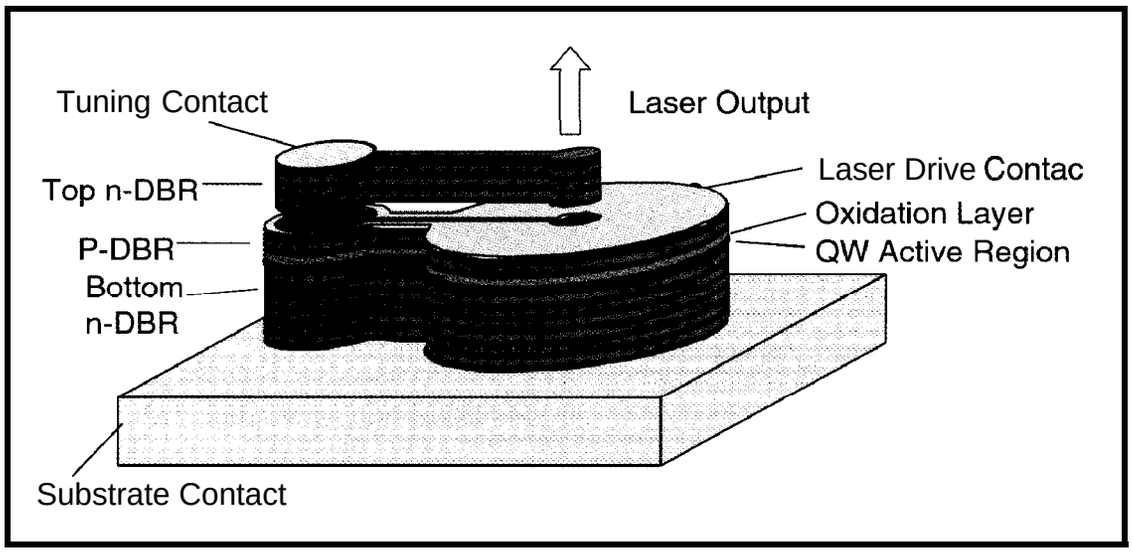

Figure 2. Schematic cross section of Bandwidth9's 1.5 μm single-epitaxy tunable VCSEL, which allows a temperature-Independent lasing wavelength and temperature-stable lasing threshold current (compared to GaInNAs/AlGaAs heterostructures, which have a wavelength limit of 1.3 pm).

Progress on 1.55 pm VCSELs has been hindered by poor optical and thermal properties at this wavelength.

Dr C J Chang-Hasnain, Bandwidth9 Inc

the thermal resistance. The p-InAlAs confinement layer is thin (about 50 nm) for small thermal conductivity.

For 1.55 μm VCSELs, a diameter of 17 μm gave cw optical output power at 20°C of a record 2 mW with a threshold current of around 5 mA. A 5 urn-wide VCSEL achieved a maximum output power of 0.5 mW with a threshold current of 0.5-0.7 mA.

For 1.8 μm VCSELs, threshold currents were 0.2 mA (2.5 μm diameter) and 3.5 mA (22 μm). The maximum temperature for cw operation is 70-90°C.

Emission at a wavelength of 2 μm is feasible, concludes Amann.

Top-emitting, integrated-MEMS-tunable 1.55 pm VCSELs

Nevertheless, C J Chang-Hasnain of Bandwidth9 Inc (Fremont, CA, USA) says progress on 1.55 μm VCSELs has been hindered by poor optical and thermal properties at this wavelength.

Tunnel-junction injection in conjunction with (i) a metamorphic distributed Bragg reflector (DBR), (ii) a dielectric DBR, or (iii) AlGaAsSb DBRs can yield good cw operation, but all three approaches rely on the heat sinking provided by flip-chip packaging, which is suitable only for bottom-emitting VCSELs.

However, a top-emitting structure is essential for practical products, since:

(i) it is the only geometry that has proven reliability (most likely because the active region and the DBRs are situated far from the solder joint);

(ii) it facilitates wafer-scale testing and processing, and improves coupling efficiency into a single-mode fibre; and

(iii) it facilitates easy integration with a MEMS structure for wavelength tunability.

Chang-Hasnain reported what is claimed to be the first electrically pumped, directly modulated, top-emitting tunable VCSELs with continuous, repeatable and hysteresis-free tuning over 1530-1620 nm wavelength. It is also the first top-emitting 1.5-1.6 μm laser grown by a single epitaxy step operated up to 550°C cw and with output power of as high as 0.5 mW at 25°C.

Bandwidth9's VCSELs have a lattice-matched n-InAlGaAs/InAlAs bottom DBR, an InGaAs

Fujitsu expects 10% shrinkage in optical transport in 2001

In the first plenary talk at IPRM, Masumi Fukuta of **Fujitsu Quantum Devices Ltd** gave Fujitsu's revised forecast for the worldwide optical transport market. Last November **RHK Inc** forecast 46% growth from US$28bn in 2000 to US$41bn in 2001 then 25% growth per year to US$75bn in 2004.

Fujitsu predicts 10% shrinkage to US$26bn in 2001 (though still growing slightly outside the US). Growth will resume at 25% per year from 2002 but now to only US$50bn in 2004.

If the market for components (e.g. DFB lasers, detectors and pump lasers) is 10% of this, then instead of growing from US$2.8bn in 2000 to US$4.1bn in 2001 then US$7.5bn in 2004, Fujitsu reckons that the component market will shrink to US$2.6bn in 2001 then grow to US$5bn in 2004.

GaInNAs allows long-wavelength lasing on a GaAs substrate (e.g. at 1.3 μm) with excellent electron confinement in the active region due to a high conduction-band offset with GaAs barriers.

This gives excellent Peltier-free high-temperature performance (with T_0 = 127-274K) as well as monolithic integration with AlGaAs-based DBRs with high reflectivity and thermal conductivity for VCSELs.

quantum well (QW) active region, a GaAs/AlGaAs DBR structure grown metamorphically on an InP substrate (to relax the constraints imposed by lattice matching and allow high-reflectivity and direct current injection simultaneously), with selective oxidation for electrical and optical confinement as well as a monothically integrated cantilever-supported movable DBR (i.e. a cantilever-VCSEL).

The top mirror consists of three parts (from the substrate side - see Figure 2): a p-DBR, an air-gap, and a top n-DBR (suspended above the cavity by the cantilever). Tuning is therefore continuous, repeatable and (since the cantilever movement is elastic) hysteresis-free. This enables "dark tuning" (where the transmission system can lock on to a channel ahead of data transmission). This is crucial for reconfigurable Metro Area Networks, when activation and re-direction of a broadband optical signal must be accomplished without interference to other operating channels.

The current tuning range is in the C-band, but Bandwidth9 expects to tune over the entire C- or L-band with a simple variation of design. (The next-generation will be for both C- and L-bands.)

The VCSELs can be directly modulated at 2.5 Gb/s (for OC-48) over 150 km of single-mode fibre and have a >45 dB side-mode suppression ratio, making them promising for reconfigurable Wavelength Division Multiplexing (WDM) Metropolitan Area Networks.

2. Temperature-stabilised long-wavelength lasers

First GaAs-based 1.55 μm GaInNAs/GaAs lasers

A problem with InGaAsP/InP lasers for WDM systems is the fluctuation of wavelength with ambient temperature due to the temperature dependence of the InP bandgap, necessitating Peltier coolers.

In contrast, InGaAsN allows long-wavelength lasing on a GaAs substrate (e.g. at 1.3 μm) with excellent electron confinement in the active region due to a high conduction-band offset with GaAs barriers. This gives excellent Peltier-free high-temperature performance (with a characteristic temperature of T_0 = 127-274K) as well as monolithic integration of AlGaAs-based DBRs with high reflectivity and thermal conductivity for VCSELs.

M Fischer, D Gollub and A Forchel of the University of Würzburg and M Reinhardt of nanoplus Nanosystems and Technologies GmbH (Würzburg, Germany) reported ***the first 1.55 μm GaInNAs/GaAs lasers.*** These were grown by Solid-Source MBE (SS-MBE) with an RF plasma source for the generation of active nitrogen, using a custom-designed shutter to give abrupt hetero-interfaces between N-containing and N-free layers. The compressively strained single quantum wells (SQWs) were implemented in the active region of separately confined heterostructure (SCH) lasers.

The optimum growth temperature was found to be 450-470°C, but subsequent layers grown at higher temperature (GaAs at 590°C, AlGaAs cladding layers at 680°C) may cause an annealing effect.

Test structures with N = 1.5-2% showed photoluminescence at 1.3 μm; those with In = 38% and N = 5.3% showed PL at 1.55 μm.

A 600 x 4 μm SQW ridge waveguide lasing at 1291 nm (with GaAs barriers considered to be a better choice than N-containing barriers) showed thresholds of 2 1 mA under cw operation at room temperature with efficiencies exceeding 0.5 W/A. It can be operated cw up to 120°C. AT, of about 160K was obtained under pulsed operation up to 100°C. The wavelength shift with temperature was typically 0.34 nm/K (which is less *than for InP*).

For laterally coupled DFB lasers, single-mode emission at 1280-l 370 nm was achieved under cw operation (the latter wavelength is of interest for gas sensing applications). The wavelength shift with temperature is 0.07 nm/K (low

Figure 3. Threshold current density versus inverse cavity length for GaNAs- and GaAs-barrier 1.3 1 pm GaInNAsSb lasers.

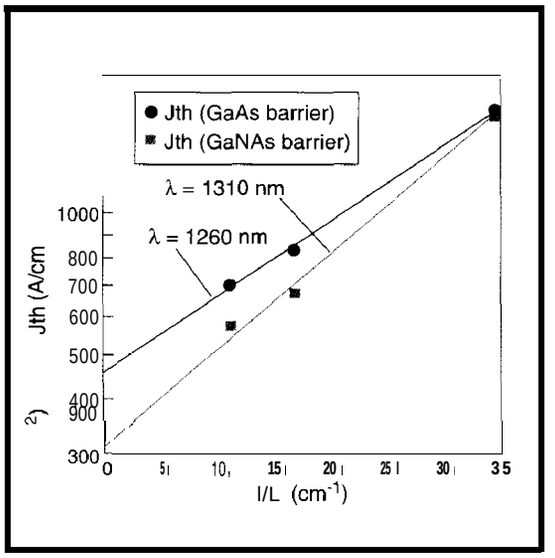

compared to InGaAsP). Thresholds of uncoated lasers can be as low as 29 mA at room temperature with external quantum efficiencies of 0.16 W/A per facet and side-mode suppression ratios of around 45 dB.

For 1.5 μm ridge-waveguide lasers, pulsed operation of a double quantum well has been achieved up to 80°C (e.g. for a 780x2 μm cavity and pulse width of 300 ns at a period of 1 ms, the room-temperature threshold current was 530 mA with a slope efficiency of 0.1 W/A). The emission wavelength is 1513 nm ***(among the highest achieved for InGaAsN)*** and the wavelength shift with temperature is 0.46 nm/K (less ***than for InGaAsP***).

Improved crystal quality by using GaInNAsSb

However, the crystalline quality of GaInNAs is still poor for laser applications. A possible solution is the use of surfactant. In particular, Furukawa Electric's Yokohama R&D Labs reported cw operation of 7.3 nm-thick, highly strained Gas-Source MBE-grown (GS-MBE) $Ga_{0.61}In_{0.39}N_{1-y1-y2}As_{y1}Sb_{y2}$ SQW active layers with 250 nm-thick InGaP cladding layers and 130 nm-thick GaAs SCH layers. Here the small amount of Sb acts as a surfactant on the GaAs substrate to improve the crystalline quality, increasing the critical thickness at which the growth mode changes from 2D to 3D.

Ridge lasers with cavity length L=200 μm and facet reflectivities of 78% and 95% under cw operation gave threshold current I_{th}=12.4 mA at 25°C (almost equal to the best reported figures for narrow-stripe edge-emission lasers) at a lasing wavelength of 1.258 μm with T_0=157K at 25-85°C (the best result for InGaAs-based edge-emission lasers). Slope efficiency at 25°C is also high (0.22 W/A).

Furukawa Electric also grew 1.31 μm lasers with a 7.3 nm-thick $Ga_xIn_{1-x}N_{1-y1-0.016}As_{y1}Sb_{0.016}$ he same assingle quantum well (with In=1-x=0.35, 0.37, 0.39 and N_2 flow rates = 0.05-0.15 ccm) and 250 nm InGaP cladding layers by GS-MBE and observed the dependency of the PL on increasing N composition in the well layer.

PL showed that N was incorporated linearly up to 0.9% and that wavelength increased with In composition and N_2 flow rates, reaching 1.34 μm for In = 0.37 and N = 0.15 ccm. However, N incorporation rates decrease with increasing indium concentration (probably caused by the weakness of the In-N bond compared to the Ga-N bond). PL intensities were an order of magnitude weaker for 1.3 μm lasers than for 1.2 μm lasers (regardless of composition or annealing conditions).

To overcome deterioration of PL intensity, the barrier material was changed from 130 nm SCH GaAs to 100 nm SCH GaAs layers with 30 nm GaNAs barrier layers (for which nitrogen incorporation rates were twice those for the $Ga_xIn_{1-x}N_{1-y1-0.016}As_{y1}Sb_{0.016}$ films). The PL wavelength is longer for GaNAs barriers since there is a smaller conduction-band offset than for GaAs barriers, resulting in smaller quantization energy. PL intensities are comparable as-grown, but much greater for GaAsN barriers than for GaAs after annealing, showing greater crystalline quality (perhaps due to the homogenous-like junctions). PL at 1.3 μm with the same intensity as 1.2 μm lasers was obtained from $Ga_{0.63}In_{0.37}N_{0.009}As_{0.975}Sb_{0.016}/GaN_{0.018}As_{0.982}$ SQW layers after annealing at 650°C.

Broad contact 1.308 μm lasers of this composition gave very low threshold current density J_{th} of 570 A/cm² for a 900 pm-long cavity under pulsed operation at room temperature ***(almost equalling the best GaInNAs lasers over 1.29 μm)***. Unfortunately, the gain coefficient is 1300 cm^{-1} for GaNAs barriers compared to 1700 cm^{-1} for GaAs, so T_0 is reduced 13%. Hence, further characteristic temperature optimization of composition or barrier structure is necessary.

GaInNAs by MOCVD with low threshold current

Compared to GaInNAs/GaAs lasers grown by MBE, MOCVD has generally given higher threshold currents and broader PL emission. However, the Royal Institute of Technology (Kista, Sweden) and Mitel Semiconductor AB have shown that a broad-area GaInNAs QW laser emitting at 1.3 μm grown by MOCVD (between 140 nm SCH layers and 1.6 μm AlGaAs cladding layers) - in the limit of very low growth rate (0.03-0.04 nm/s) and temperature (475-505°C) - retains constant and high PL emission from 1175 nm up to 1210 nm (although from 12 10 to 1350 nm the intensity drops rapidly by three orders of magnitude due to the onset of strain relaxation mechanisms).

Although PL full-width-half-maximum (FWHM) decreases with increasing temperature (possibly indicating improved interface quality), the intensity decreases with temperature (a factor of three lower at 495°C than at 475°C). However, the 1280 nm laser grown at 495°C has a significantly lower threshold current density than the 1290 nm laser grown at 475°C (0.8 kA/cm² compared to 2 kA/cm²). This suggests that the FWHM is a more important parameter for predicting laser performance (where composition and

The emission wavelength is 1513 nm (among the highest achieved for GaInNAs) and the wavelength shift with temperature is 0.46 nm/K (less than for InGaAsP).

University of Würzburg and nanoplus Nanosystems and Technologies GmbH

Broad contact 1.308 pm lasers of this composition [GaInNAsSb] gave very low threshold current density J_{th} of 570 A/cm² for a 900 pm-long cavity under pulsed operation at room temperature (almost equalling the best GaInNAs lasers over 1.29 pm).

Furukawa Electric

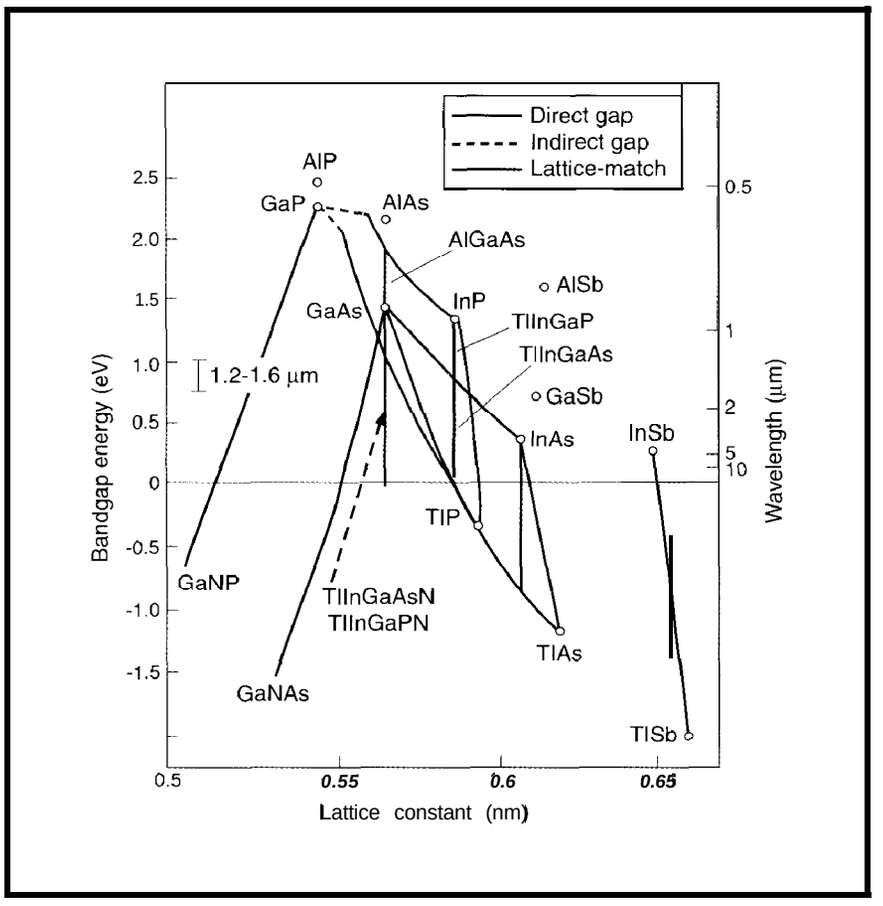

Figure 4 Bandgap energy vs lattice constant for Tl-III-V-N alloys (TlInGaP, TlInGaAs, TlInGaPN, TlInGaAsN).

wavelength are similar). Also, for a 1.2 mm cavity length, T_0 = 100K for the 495°C 1.28 μm laser and 80K for the 475°C 1.29 μm laser (not the highest reported values for GaInNAs but *higher than the 65K of InP-based devices*). The trend suggests that it could be favourable to go to higher temperature. However, so far good QW characteristics have not been obtained above 500°C.

Thallium compounds for longer wavelength and greater temperature stability on InP

GaInNAs/AlGaAs heterostructures offer lasers with temperature-stable threshold currents (due to the large conduction-band discontinuity). However, it is difficult to grow beyond a wavelength of 1.3 μm due to degradation of the crystal quality and reduction of valence-band offset with increasing N composition.

It is difficult to grow [GaInNAs] beyond a wavelength of 1.3 pm due to degradation of the crystal quality and reduction of valence-band offset with increasing N composition.

Alternatively, since TlInGaAs is an alloy of semiconducting InGaAs and the semi-metal TlAs, it has both low bandgap/long wavelength and temperature-stable bandgap energy (similarly with InGaP and TIP for TlInGaP, as for $Hg_{0.48}Cd_{0.52}Te$). PL from TlInGaAs and TlInGaP has previously shown temperature variations in peak energy of just -0.03 meV/K and wavelength of 0.04 nm/K.

However, TlInGaAs cannot be lattice matched to GaAs without adding nitrogen (see Figure 4). Hence TlInGaAsN/AlGaAs heterostructures are proposed for 1.3-1 .55 μm lasers with temperature-stable threshold currents and wavelengths.

Like GaInNAs/AlGaAs, heterostructures of TlInGaAsN/AlGaAs and TlGaAsN/AlGaAs also have large conduction-band discontinuity

But first Osaka University reported TlInGaAs/InP double heterostructure LEDs grown on (100) InP substrates by GS-MBE at 450°C with a Tl composition of 6% and operated at up to 340°C at about 1.58 μm. Temperature variation in electroluminescence peak energy was very low (-0.09 meV/K - similar to the temperature variation in PL).

Then, as a first step to the growth of TlInGaAsN/AlGaAs heterostructures, H J Lee *et al* of Osaka University grew comparable InGaAs and TlInGaAs/GaAs double-heterostructures (with In = 8%) by GS-MBE at 450°C (with Tl = 9%), with TlInGaAs of thickness less than 20 nm (due to the lattice mismatch) sandwiched between GaAs. Compared to InGaAs, the TlInGaAs showed a lower energy shift of the PL peak at 77K (by as much as 20 meV). However, the PL intensity from both was weak.

Multi-heterostructures were therefore grown (with In = 10% and Tl = *3%).* PL intensities were increased by several factors. A smaller red shift of the PL peak energy was seen (due to the smaller Tl composition and the increased In composition). A sharper PL spectrum was observed. However, optical qualities are still not enough for PL emission at room temperature.

3. InP electronics

InP HBTs with high breakdown voltage

The substrate transfer process has yielded InP-based single heterojunction bipolar transistors (SHBTs) with high cut-off frequencies (since it allows narrow emitter/base and collector/base junctions on opposite sides of the base epitaxial layer). However, SHBTs have low breakdown voltage and high output conductance, limiting their use in high-voltage and precision analogue circuits.

Instead, higher breakdown voltages can be achieved by using wider-bandgap InP for the collector. University of California Santa Barbara and IQE Inc reported InP/InGaAs/InP double HBTs with a 400Å-thick graded base and a 3000Å collector depletion region which yielded f_{max} = 300 GHz and f_T = 165 GHz with breakdown voltage BV_{CEO} = 6 V at a current density of J = $1x10^5$ A/cm^2.

Integrated pnp and npn complementary HBTs

So far, research on InP-based HBTs has focused almost exclusively on npn HBTs since electron velocity is several orders of magnitude higher than the hole velocity in the InGaAs channel layer.

However, pnp HBTs would enable integration with npn HBTs, acting as active loads for npn HBTs (eliminating the large resistor values and saving chip area in high-gain amplifiers) as well as allowing the design of multi-stage amplifiers with alternating npn and pnp HBTs. Also, integrated npn and pnp HBTs can form a "true" class B push-pull power amplifiers (without the need for complex 180" transformer circuits) for simultaneous improvement of both efficiency and linearity.

Most pnp HBTs reported have been InAlAs/InGaAs due to the difficulty of obtaining high p-type concentration in the emitter while keeping a low p-type concentration in the collector.

Also, monolithic integration has previously been demonstrated by uninterrupted MBE growth of pnp and npn layers on mesa-patterned substrates, resulting (in 1993) in planar technology for both HBT types. However, parasitics introduced by the pnp HBT layer (grown directly on semi-insulating InP substrate) and the semi-insulating InAlAs isolation layer (grown at low temperature) can degrade the electrical performance of the npn HBT layer stacked ontop.

Now, the University of Michigan and TRW have reported monolithic integration of npn and pnp InAlAs/InGaAs complementary HBTs grown using a selective MBE re-growth approach. A pnp structure was grown over the entire wafer then coated with an SiN mask layer at least 10 μm thick before patterning, etching and re-growth of the npn HBT structure. Hence, both planar npn and pnp HBTs are grown directly on the semi-insulating InP substrate, eliminating any isolation or parasitic problems from a semi-insulating InAlAs layer.

Compared to similar discrete devices, the monolithically integrated devices showed little degradation due to re-growth, giving DC gain = 35 for both HBTs (compared to 40 for discrete npn HBTs), f_T =79.6 GHz and f_{max} = 109 GHz for the npn and f_T =1 1.6 GHz and f_{max} = 22.6 GHz for the pnp (for 5x10 μm^2 HBTs). Performance matching could be achieved by modifying the npn structure to downgrade its performance or (preferably) designing the biaising circuits to make the npn devices work less optimally to match the pnp performance (leaving circuits on the same wafer that use only the npn HBTs unaffected) as well as intentionally mismatching for npn devices in the npn-pnp circuits.

The University of Michigan also claims the first InP/InGaAs pnp HBT grown by MOCVD. (The only one reported so far was grown by metall-organic-MBE (MOMBE), yielding a gain of 20 and f_T = 10.5 GHz and f_{max} = 25 GHz for 3 x 8 μm^2 emitters.) A zinc-doped InP layer was used as the emitter and a 500Å-thick n-type InGaAs layer doped at at $5x10^{18}$ cm^{-3} as the base. The growth temperature was 570°C.

A 1x20 μm^2-emitter HBT showed DC gain of more than 10 and at $J_c = 8.25x10^4$ A/cm^2, an f_T of 11.2 GHz and f_{max} = 8.1 GHz. The latter was lower than MOMBE due to the limitation of mimimum controllable p-type doping concentration to high 10^{17} cm^{-3}. If the collector doping can be reduced to the desired 10^{16} cm^{-3} (equal to MOMBE) then an f_{max} of about 25 GHz is expected.

The high-frequency performance is limited by the uniform doping of the base. Compositionally graded and doping-graded bases have been used in pnp AlGaAs/GaAs HBTs. Similarly, introduction of electrical fields into the n-type base of InP/InGaAs HBTs could aid the hole transition through the base and reduce the total emitter-to-collector transit time significantly.

Single-step epi GaInNP/GaP LEDs and GaInP/GaAs HBTs

Since incorporating a small amount of nitrogen (less than 5%) in GaAs- and InP-based III-V compounds results in very large bandgap bowing, the University of California, San Diego reported on GaInNP grown by GS-MBE at 480°C on GaP or GaAs substrates for LEDs or HBTs.

Previously it was shown that adding just a small amount of nitrogen (0.5%) to GaP results in strong PL, which indicates direct-bandgap behaviour of GaNP. Now, it is shown for GaNP that PL increases with increasing N content (up to N=1.3%), contrary to GaInNAs and GaNAs. $GaN_{0.011}P_{0.989}$/GaP red (650 nm) LEDs (with a 500 nm-thick active layer, partially relaxed by 15%) showed quantum efficiency of 1-2%. This is still an order of magnitude less than commercial AlInGaP/GaAs high-brightness LEDs. However, the latter requires removal of the absorbing GaAs substrate and wafer bonding of the active layers to a transparent GaP substrate, compared to single-step GaNP epitaxy on GaP To lattice

The University of Michigan and TRW have reported monolithic integration of npn and pnp InAlAs/InGaAs complementary HBTs grown using a selective M BE re-growth approach... Both planar npn and pnp HBTs are grown directly on the semi-insulating In P substrate, eliminating any isolation or parasitic problems from a semi-insulating InAlAs layer.

It is shown for GaNP that PL increases with increasing N content (up to N=1.3%), contrary to GaInNAs and GaNAs.

University of California, San Diego

Greg Olsen of Sensors Unlimited wins Michael Lunn Award for 2001

The *Michael Lunn Award for 2001* for "*outstanding contributions to the InP community*" was awarded by the IPRM organizing committee to Dr Gregory H Olsen, founder and president of Sensors Unlimited Inc. Olsen has been involved in the exploitation of InP-based components since working at Sarnoff Labs before starting Epitaxx in 1984. In 1992 he started Sensors Unlimited, which develops InGaAs photodetectors for telecoms and photographic applications. By 2000 revenues had risen to US$25m, leading to the acquisition of Sensors Unlimited in July 2000 by Finisar Corp). In the 1970s, Olsen also pioneered the hydride VPE growth of InGaAsP alloys at RCA and made some of the first long-wavelength lasers and photodetctors.

mismatch to GaP, just a few percent of indium is incorporated to form $Ga_{1-x}In_xN_yP_{1-y}$ (x=2.23y).

The integrated PL intensities of $GaN_{0.015}P_{0.985}$ and $Ga_{0.976}In_{0.024}N_{0.016}P_{0.984}$ are four and six times that of a reference sample $Ga_{0.51}In_{0.49}P$ bulk layer, respectively. However, N complexes (including N isolated centres, N pairs and N clusters) cause potential fluctuations which induce broad PL peaks.

Also, $Ga_{0.52}In_{0.48}P$ lattice matched on GaAs has advantages over AlGaAs/GaAs structures due to a larger valence-band discontinuity, better etch selectivity, and less oxidation effect. For an npn HBT, however, the conduction-band discontinuity should be eliminated. As when adding N to InGaAs, the majority of the bandgap reduction through adding N to GaInP is expected to be through lowering of the conduction band. Therefore, $Ga_{1-x}In_xN_yP_{1-y}$ may be suitable for the emitter and collector of an npn HBT (specifically, a blocked-hole HBT, through the large valence-band discontinuity and large hole effective mass, while there would be no electron barriers at the base-collector junction).

As when adding N to InGaAs, the majority of the bandgap reduction through adding N to GaInP is expected to be through lowering of the conduction band. Therefore, $Ga_{1-x}In_xN_yP_{1-y}$ may be suitable for the emitter and collector of an npn HBT.

University of California, San Diego

For a set of S-period $Ga_{0.46}In_{0.54}N_yP_{1-y}$(20nm) /GaAs(5nm)/$Ga_{0.46}In_{0.54}N_yP_{1-y}$(20nm) MQW samples, there was no GaAs QW PL emission when the barrier has a higher N concentration (e.g. 1.2% and 2.4%). This is possibly because high N composition decreases the $Ga_{0.46}In_{0.54}N_yP_{1-y}$ too much and $Ga_{0.46}In_{0.54}N_yP_{1-y}$/GaAs has a type II alignment (such that the electron and hole separation results in much weaker PL). Using a finite-barrier quantum well model with the experimental PL data, the conduction- and valence-band discontinuities AE, and ΔE_v for $Ga_{0.46}In_{0.54}P$/GaAs were calculated as (42±3)% and (58±3)% of the total bandgap difference (404 meV), respectively (similar to previous reports based on C-V profiling). With 0.5% incorporation into the barrier, these become (3±1)% and (97±1)%, respectively, so $Ga_{0.46}In_{0.54}N_{0.005}P_{0.995}$ should be ideal for HBT emitters or collectors. (Currently, GaInP/GaAs HBTs are being fabricated with a thin GaInNP hole-blocking layer in the collector.)

InP HEMTs for 40 Gb/s

Fujitsu presented thermally stable InGaAs/InAlAs/InP HEMTs (which can have an f_T over 300 GHz) grown by MOCVD on 3" InP wafers. These have uniform offset-voltage in high-gain differential amplifiers (commonly used in digital circuits such as mux/demux) with standard deviation of only 6.2 mV and threshold voltages V_{th} which change by less than 11 mV when annealed for 60 minutes at 330°C (essential for thermally stable 40 Gb/s operation) through better uniformity of the gate and the recess region than reported previously (by passivating the InP etch-stop layer on the recess region entirely by using dielectric film).

While most reliability data for InGaAs/InAlAs/InP HEMTs have been for discrete devices only, TRW presented the first report of high-reliability 0.1 μm-gate InGaAs/InAlAs/InP HEMT MMICs based on small-signal microwave characteristics (using a high-volume production process technology on 3" InP substrates for K-band MMICs).

CNRS France and Universidad de Salamanca reported InGaAs/InAlAs/InP HEMTs (grown by MBE) for both a 60 nm-gate standard structure (designed for 100 nm-gate HEMTs) with an aspect ratio of gate length over gate-to-channel distance (L_g/A) of just 3 and a 70 nm-gate optimised structure (designed for 50 nm-gate HEMTs)

with $L_g/A=4.5$, e.g. by reducing A to 11.5 nm (to reduce short-channel effects). This yielded comparable f_T but f_{max} of 260 GHz and 470 GHz, respectively. The gate-to-channel distance cannot be reduced any further because of gate tunnelling current and depletion from the surface of the carrier in the channel near the recessed region.

To improve Schottky characteristics and the confinement of electrons in the channel, Al content in the InAlAs layers was increased from the standard 52% to 65%. To improve carrier transport properties, In content in the channel is also increased from the standard 53% to 65%.

For a sub-50 nm-gate optimized structure an f_T of >300 GHz and f_{max} of >600 GHz are expected.

First sub-O.1 pm MHEMTs yield record 260 GHz

Future communications systems will require devices with f_T and f_{max} > 300 GHz. A 50 nm-gate InP-based HEMT was reported with f_T = 362 GHz.

However, an aim is to develop comparable HEMTs grown metamorphically on larger, less expensive GaAs substrates using InGaAs, InAlAs or AlGaAsSb buffer layers. Al-containing buffers are preferred to indium because of the high electrical isolation.

$In_{0.5}Ga_{0.5}As/In_{0.5}Al_{0.5}As$ metamorphic HEMTs grown by MBE on GaAs have shown higher f_{max} than InGaAs/InAlAs HEMTs lattice-matched on InP. However, problems include instability due to the easily oxidized InAlAs around the gate and low breakdown voltage due to the small bandgap of the InGaAs channel.

In lattice-matched InGaAs/InAlAs/InP HEMTs grown my MOCVD, the oxidation problem has been solved by using an InP capping layer, while the breakdown voltage has been improved by using an $In_{0.5}Ga_{0.5}As/InP$ composite channel.

Now, K Ouchi, T Mishima, M Kudo and H Ohta of Hitachi have reported the first MHEMTs grown by gas-source MBE, and with not only an InP capping layer (for long-term reliability) but also an $InGaAs/InAs_xP_{1-x}$ composite channel layer (with x varied from 0.12 to 0.3).

The InAsP sub-channel was adopted because of its low conduction-band edge discontinuity (AE,) of the InGaAs/InAsP heterointerface, in which hot electrons can be transferred easily from high-mobility InGaAs to high-saturation-velocity, wider-bandgap InAsP. For such a complicated structure, GS-MBE was chosen because it can be done at low temperature and it can control the compositional ratio of As and P precisely

First, a step-graded buffer layer was grown, but the mobility could not match SS-MBE. However, a 0.45 µm linear-graded buffer yielded a room-temperature mobility of over 9000 cm^2/Vs (comparable to Solid-Source MBE) when the As composition of the InAsP sub-channel layer was less than 0.2 (for which AE, is minimal) and the growth temperature was 350-400°C (almost the same for SS-MBE growth of MHEMTs). The InP etch-stop layer enabled satisfactory gate-recess etching.

In late '99, K C Hwang et *al* reported 0.1 µm-gate InGaAs/InAlAs HEMTs on GaAs with f_T = 225 GHz. Now CNRS France has reported the first sub-o.1 µm MHEMT on GaAs – a $In_{0.57}Ga_{0.47}As/In_{0.52}Al_{0.48}As$ MHEMT with a 60 nm-gate (and a 1.3 urn-thick graded buffer - with an indium composition from x = 0.01 to 0.62 – grown at 400°C followed by a 0.3 µm inverse step of x = 0.52 grown at 500°C). f_{max} is 490 GHz (i.e. little-affected by shortchannel effect) and f_T = 260 GHz, "the highest frequency performance ever reported for HEMTs on GaAs". Room-temperature mobility was 9180 cm^2/Vs. Typical drain-to-source current I_{ds} was 600 mA/mm; peak extrinsic transconductance was 850 mS/mm.

For further information or a copy of the IPRM'01 proceeedings, see http://www.knt-ec.com/IPRM01/

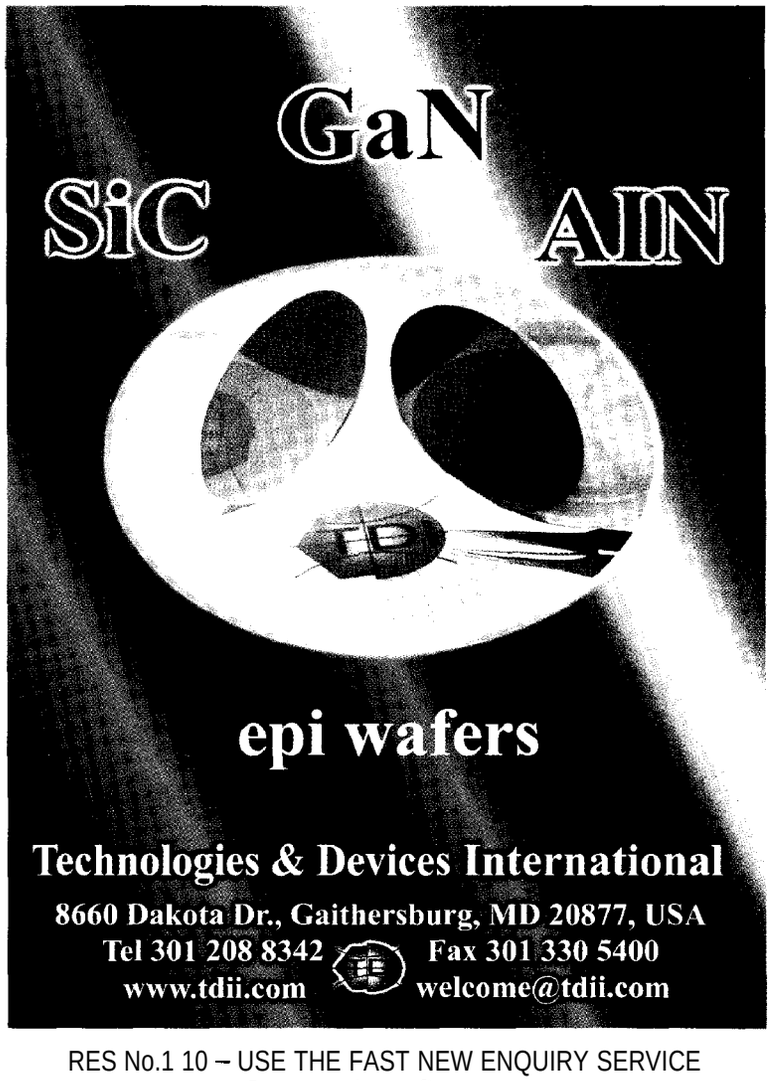

RES No.1 10 – USE THE FAST NEW ENQUIRY SERVICE
@ www.three-fives.com